Learning and Nonlinear Models – Revista da Sociedade Brasileira de Redes Neurais, 1, 1, 11-31, 2002

A NEW NEURAL NETWORK CONCEPT FOR THE CONTROL OF NUCLEAR REACTOR SYSTEMS

Benedito D. Baptista Filho[1] **Eduardo L. L. Cabral**[2]
[1] Instituto de Pesquisas Energéticas e Nucleares (IPEN-CNEN/SP)
[2] Escola Politécnica da Universidade de São Paulo
bdbfilho@net.ipen.br elcabral@usp.br

Abstract – The novel approach to artificial neural networks based on the design of task-specific networks and on biological models of a neuron with multiple synapses developed by Baptista, Cabral and Soares (1998) was extended to accommodate external perturbations. The learning algorithm of this artificial neural network is an unsupervised training method based on the processes of habituation, sensitization and classical conditioning of human reflexes. In this paper, this new development is applied to the control of the fluid temperature at any point in a natural circulation loop. The learning and the action processes were implemented in a computer program. The thermal-hydraulics processes were also simulated. The natural circulation loop simulation model is based on physical equations and on experimentally identified parameters. The results show that besides the excellent learning capability and generalization, the new improvements are suitable to accommodate external perturbations so that the network is able to maintain the controlled variable within allowable limits even in the presence of strong perturbations.

Index Terms – Artificial Neural Networks, Unsupervised Learning Algorithms, Adaptive Control.

1. INTRODUCTION

The purpose of this work is to present an improvement in the new concept of artificial neural networks introduced by Baptista, Cabral and Soares (1998) [1]. This new neural network concept, called MULSY Neural Network (Multiple Synapses Neural Network), is based on the design of task-specific networks and on biological models of a neuron with multiple synapses. In previous works, this basic neural network controller was used to control a planar two-link manipulator. That control unit was improved here to deal with external perturbations that affect the control task.

A thermal-hydraulic system was used as the control object in this paper. This system consists on a Natural Circulation Loop (NCL), which resembles an Advanced Pressurized Water Reactor Decay Heat Removal System. The NCL problem is very non-linear and due to the complexity of its functions it represents a difficult control problem. Comparing the NCL with a manipulator arm both are non-linear but their dynamic behavior is quite different, the NCL is more complex but it is much slower than the manipulator. This system of different nature was chosen to show the capability of the MULSY Neural Network to deal with different kinds of problems and situations related with external perturbations.

This paper consists of six sections. The first section is this introduction. The second section reviews the basic principles of the MULSY concept. The third section describes the Natural Circulation Loop and the dynamic model used to simulate it. The fourth section presents the development of an application of MULSY in the control of the NCL and also shows the improvements added to the basic control unit. The fifth section is devoted to show the results. The sixth section presents the main conclusions.

2. THE MULSY CONCEPT

Artificial Neural Networks (ANN) consist of regular arrays of units, *representing neurons*, interconnected by single connections with linking weights, *representing synapses*. In the last years some researchers have focused on the limitations of this approach. Kolen and Goel (1991) [2] reported results of tests conducted to identify the power and limitations of the back-propagation algorithm. They concluded that: first, *the experiment on learning suggests that the computational efficiency depends on the initial weights in the network*; second, *the information content of what is learned is dependent on the initial abstractions in the network* and third, *the learning task addressed by connectionist methods is computationally intractable*. In addition, their results indicate that current connectionist methods may be too limited for the task of learning they seek to solve, and they propose that the development of task-specific connectionist methods may enhance the power of neural networks.

The development of MULSY tries to solve some of these problems. It was based on the following principles: 1) an ANN shall be based on biological systems to take the profit of their evolutionary nature; 2) the ANN shall represent what it knows and what is to learn and must have capabilities to generalization, therefore it must have different parts specialized for different functions; 3) an ANN must be robust to missing information, incorrect data and unit removal or malfunction; 4) the learning task shall be done in real-time while functioning and shall be independent on the initial unit strength; and, 5) the process of learning and functioning must be computationally efficient without limiting the power of connection's transfer functions to obtain higher classes of input-to-output relations. To deal with these principles, a search program on biological neural systems was conducted. This search was focused on the following items: a) *architectural design and flow of information in the brain;* b) *neural signaling;* and, c) *learning and memory mechanisms.*

2.1 Architectural design and flow of information

The functional, organizational, and developmental principles of neural circuits, that make the principles of parallel processing, suggest that a control circuit must have two separated pathways, one for the upper level control commands: *the wish* -like a target position; and, the second for the sensory signals: *the present status* -as the present position. Such circuits should also have convergent pathways from the upper level and sensory systems to the motor units. Figure 1 resumes these main ideas with *a) error feedback (to maintain or correct posture); b) separated pathways for upper level control signals and sensory signals; and, c) convergence to the motor units.*

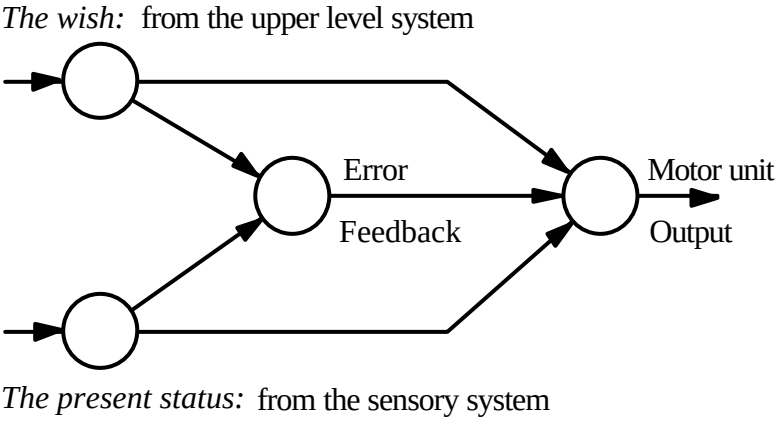

Figure 1 - Basic Structure of a Control Unit.

2.2 Neural signaling

The transfer function

The signal processing inside a neuron is a composition of the integration processes of incoming signals, generation of action potentials and conduction to other cells. The neuron's transfer function in biological systems is simple and can be generalized regardless of its size or shape. Because of this biological peculiarity, the evolutional process had to build expert systems to extend the range of functions. Akazawa and Kato (1990) [3] show a good example of this proposal. They presented a model to investigate neural mechanisms of force control based on the "size principle of motor unit." This example, associated with the "common drive hypothesis" of DeLuca et al. (1982) [4], shows that besides the number of units has important role in terms of robustness it is also essential to the *meaning of the signals*. Artificial neural networks do not have the same constraints of biological systems. Because of this, an unit transfer function improvement can reduce the number of units, reducing computation usage. A single unit with a transfer function in a real domain can emulate the effect of agonist and antagonist circuits of biological systems. The benefits of the size principle of motor units can be used defining the *unit size (T_N)*. The resulting transfer function is a modified hyperbolic tangent function expressed by:

$$O = T_N \tanh\left(\alpha \sum S\right) \tag{1}$$

where O is the output signal; T_N represents the "size" of the unit; α is a gain; and ΣS is the summation of all synaptic input to that unit. The "size" can be set to convenient values to improve the linearity in the range of interest or to amplify or reduce the input to output relation.

Synaptic transmission modeling

Synaptic transmission depends on several processes in the nerve terminals that are even important for the cell survival. According to Kandel, Siegelbaum, and Schwrtz (1991) [5] an average neuron forms about 1000 synaptic connections and receives even more; a motor neuron may have 10,000 different presynaptic endings and a Purkinje cell receives around 150,000 contacts - *about 10^{14} synaptic connections are formed in the brain*. This fact gave the idea of improving the ANN concepts with the "*multiple synapses model.*" The multiplicity of synapses can improve the overall transfer function capability, increasing the connective complexity but reducing the overall number of units.

In these biological synaptic contacts, chemical synapses predominate. With this kind of synapses *the most remarkable activities of the brain such as learning and memory* are associated. In the chemical synapses, transmitters released from presynaptic terminals process the signaling as a function of the incoming signals. The transmitter released acts on a large number of ions' channels: *the receptors of the target cell*. The number of activated channels opened during the synaptic potential is limited by the amount of transmitter available. The chemical transmission has the properties of amplification and attenuation. A Gaussian like function is suitable to represent the neural synaptic transmission process:

$$S = \frac{T}{1 + a(I - I_0)^2} \tag{2}$$

where T is the "strength" of the synapse, which can be set as any positive value (excitatory) or as any negative value (inhibitory); a is a constant; I is the signal value that pass through the axon; and, I_0 is the value of I, which is called "threshold," that maximizes S, the output value to the target cell.

An example of the shape of this function is shown in Figure 2. This function has the properties of amplification, attenuation and selective response, as would occur during synaptic formation according to the resonance hypothesis of Paul Weiss (1948) [6]. Also, it enhances the whole unit transfer function capability and mimics the stochastic process of transmitter release through the numerous ion channels present in the synaptic contacts. With convenient strengths and thresholds, a set of functions like that of equation (2) can produce any kind of continuous function (Baptista – 1998) [7].

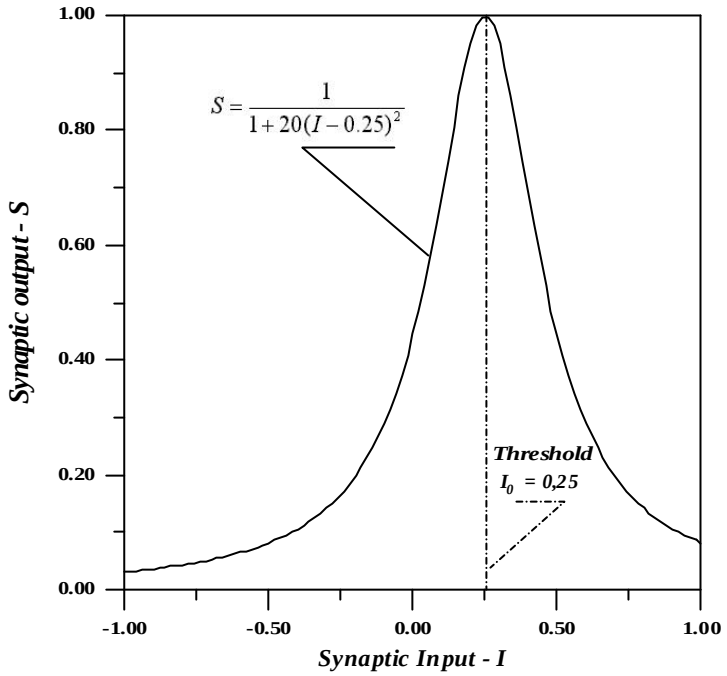

Figure 2 - Synaptic Transfer Function.

2.3 Learning and memory mechanisms

Learning is the process of acquiring knowledge about the world and memory is the storage of this knowledge. The study of memory mechanisms provides the fundamentals to implement a learning process based on biological processes. Reflexive memory is the memory that accumulates slowly through repetition over many trials. This topic reviews some aspects of the *biological learning processes* and some *physical mechanisms* of memory, and also presents how these biological processes are modeled and incorporated in the MULSY Neural Network.

Learning processes

A single set of synapses can participate in different forms of learning: *they can be depressed by habituation or enhanced by sensitization.* More complex forms of learning are *classical conditioning and practice.* Detailed studies of these processes [8, 9 and 10] suggest the design of a specific circuit to implement the learning process based on the reflexive memory mechanisms. This circuit, shown in Figure 3, scales error signals via one facilitating inter-unit connected to the output unit synaptic terminals through axo-axonic connections, where the changes are to be effected. The sign of the error dependent signal decides if the process is a presynaptic facilitation or presynaptic inhibition, which will increase or decrease the synaptic strength.

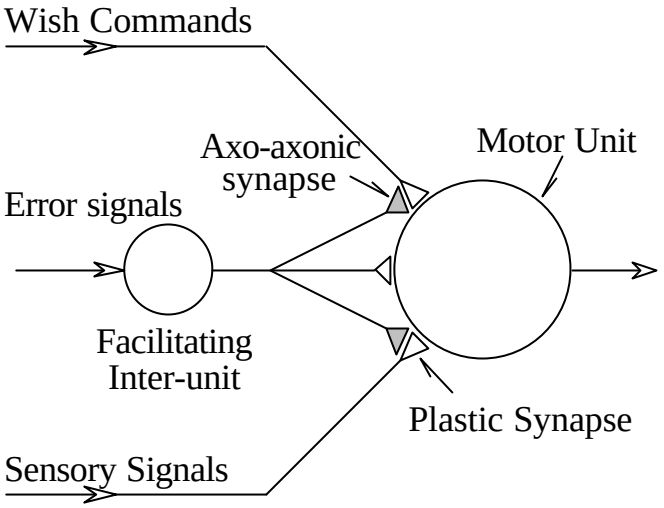

Figure 3 - Synaptic array for the Learning Process.

Mechanisms of memory storage

A plasticity model based on memory storage mechanisms can outfit the modification of the synaptic strength during the learning process. Memory storage does not depend on *dynamic changes* in a closed chain of neurons, but on *plastic changes* in the strength of preexisting connections. These plastic changes are not a feature of all synapses. Some synaptic connections in the nervous system do not change their strength at all with repeated activation. Reflexive learning does not depend on specialized memory neurons either, but instead memory storage results from changes in neurons that are integral components of a normal reflex pathway. Cellular studies indicate that a long-term storage process appears to be a graded extension of short-term processes. Furthermore, the type of contact determines the function of the synaptic connections, and this is essential to the learning mechanisms - *there are three main types of contact between cells: axo-axonic, axosomatic and axodendritic*. Axo-axonic synapses play an important role because they can depress or enhance transmitter release through presynaptic inhibition or presynaptic facilitation - *by the regulation of free Ca^{++} concentration in the presynaptic terminal*. This is the basis for a variety of mechanisms that give plasticity to chemical synapses. Aside from a modulatory influence on voltage-gated ion channels, the intracellular concentration of Ca^{++} triggers biochemical and morphological changes in the pos-synaptic cell.

The action of the facilitating inter-unit, *the presynaptic cell*, over the presynaptic contact of the motor unit, *the learning cell*, is to increase a source term - *as the Ca^{++} concentration in real cells* - that acts on the long-term plasticity. This can be modeled by a cumulative process where the governing term is proportional to the incoming signal, *the training signal* $\boldsymbol{d}$, and its decay rate:

$$\frac{dC}{dt} = T_C \boldsymbol{d} - \boldsymbol{l} C \qquad (3)$$

where C is the long-term learning factor; $\boldsymbol{d}$ is the output signal of the facilitating inter-unit; $\boldsymbol{l}$ is a decay constant; and, T_c is the strength of the facilitating synapse that controls the rate of change.

The long-term learning factor (C) can grow in a rate proportional to the learning signal ($\boldsymbol{d}$) up to an equilibrium value. This makes the change in the synapses strength faster or slower. If the incoming learning signal decreases to zero the long-term learning factor will also decrease to zero, according to the rate established by the decay constant (λ). This means that after a reasonable period of training, when the

error disappear, there will be no need for further changes, thus making the process inherently stable. To complete this idea, an artifice that makes the changes occur mainly in the convenient synapses is set, i.e., the synapses where the threshold (I_0) is closer to the incoming desired values, like in the resonance hypothesis of Paul Weiss (1948) [6]. This novel characteristic makes the correct synaptic selection. The model that establishes the strength rate of change of the synapses (parameter T in equation 2) as a function of the long-term learning factor and of the synaptic threshold is:

$$\frac{dT_j}{dt} = \frac{C}{1 + a_S (I - I_j^0)^2} \tag{4}$$

where T_j is the strength of the *j-th* synapse of the motor unit; a_s is the constant of the Gaussian like function of the facilitating synapse; I is the signal value that comes from the upper control level (the Wish); and, I_j^0 is the threshold of the synapse.

In the model described above, equation (3) emulates the process of Ca^{++} accumulation within the synaptic terminal, creating a source term that triggers the long term changes. Equation (4) selects the correct synaptic terminal (*as in the resonance hypothesis of Paul Weiss*) and yields the rate of change of the synaptic strength. This process acts on all synaptic contacts in the target unit but, with a higher strength growing rate in the synapses that have the threshold closer to the input desired signal ($I \approx I_j^0$).

2.4 Motor Control Unit concept

With the inclusion of the details needed to the learning and control tasks, the basic structure of the new neural network presented in Figure 1 was detailed to reach the structure represented in Figure 4. This figure shows a sketch that represents the "motor control unit," (MCU) which the MULSY network is based on. The input pathway from the upper level system ("The Wish" - I_c) and that from the sensory system ("The Actual Condition" - I_s) converge to the unit responsible for sensing the actual error (e) and to the motor unit. These signals are linked to the error sense unit with rigid connections that will not change with training. These connections are modeled to make the error unit to sense the actual condition from the sensory system with the opposite sign of the wish signal, i.e., $e = I_c - I_s$. The scheme of multiple branches of synaptic terminals improves the reliability as long as it allows the increase in the number of terminals making a more fail-proof system.

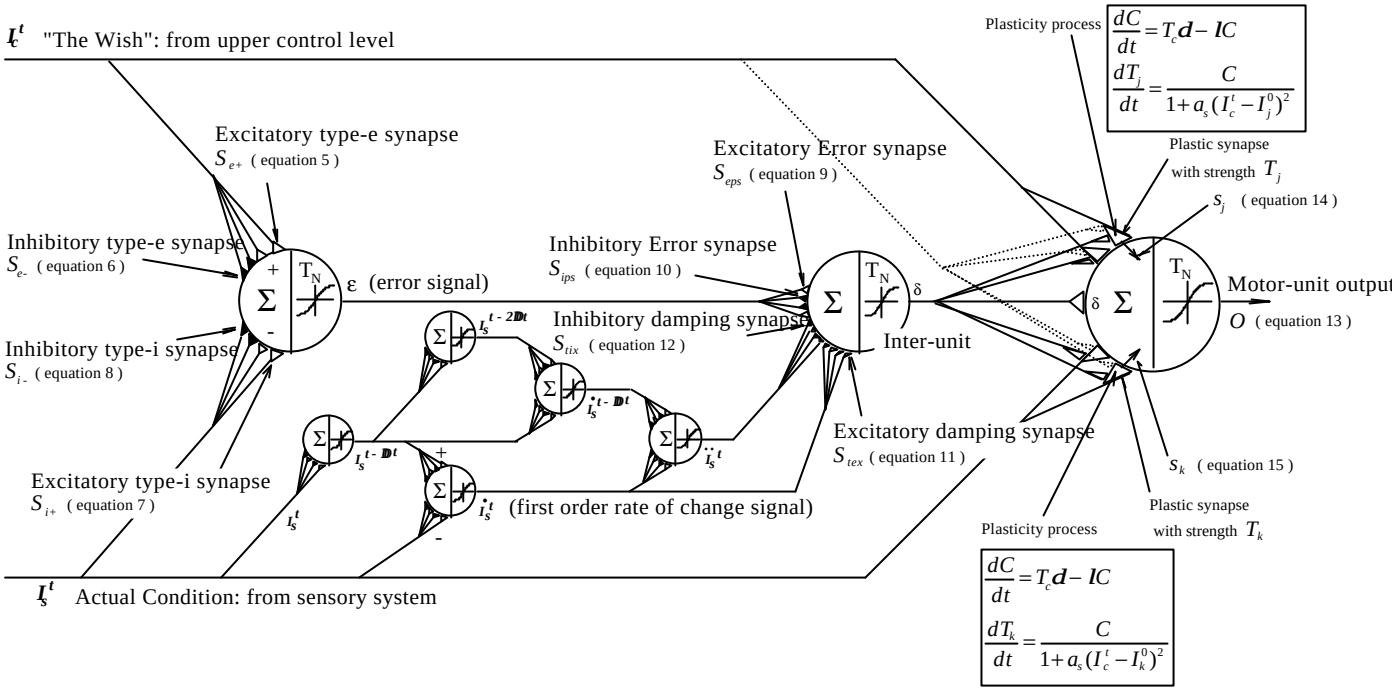

Figure 4 - Motor Control Unit of the MULSY Neural Network.

The following equations were used to model the terminal types, S_{e+} , S_{e-} , S_{i+} e S_{i-} , indicated in Figure 4:

$$S_{e^+} = \frac{1}{N}\left(\frac{2}{1+0.25(I-2)^2}\right); \tag{5}$$

$$S_{e^-} = \frac{1}{N}\left(\frac{2}{1+0.25(I+2)^2}\right); \tag{6}$$

$$S_{i^+} = \frac{1}{N}\left(\frac{-2}{1+0.25(I+2)^2}\right); \tag{7}$$

$$S_{i^-} = \frac{1}{N}\left(\frac{-2}{1+0.25(I-2)^2}\right); \tag{8}$$

where N is the number of redundancies, which does not modify the net result, the subscript e refers to the excitatory synapses, and the subscript i refers to the inhibitory synapses.

An artifice is used to sense the rates of change of the sensory signals within the network: *the differences between signals from units in different layers*. The inter-units responsible for this function are presented between the error signal and the actual condition signal of Figure 4. These units are coupled with rigid connections (which do not change during training) like that of the error unit defined previously. The output signals of these units in the several levels represent the rates of change of sensory signals. These signals are equivalent to the rate of change of the error signal when the desired value is constant. These signals are combined to the error signal into one intermediate unit that makes the connections with the output unit. This signal combination represents the system dynamics as an analogy to the summation of a_0

$\varepsilon + a_1 \, d\varepsilon/dt + a_2 \, d^2\varepsilon/dt^2 + ...$ The coefficient a_0 of the error is implemented by the following synaptic functions:

$$S_{eps} = \frac{1}{N}\left(\frac{T_e}{1+0.25(I-2)^2}\right); \quad (9)$$

$$S_{ips} = \frac{1}{N}\left(\frac{-T_e}{1+0.25(I+2)^2}\right); \quad (10)$$

where T_ε is the strength of the error synapse.

The synaptic transfer functions for the connections of the rate of change signals with the inter-unit are modeled with damping characteristics with response like $x|x|$. This is necessary to attenuate oscillations and to make the process stable even in the presence of high rates of change. This damping is biologically plausible because we have neurons and muscle cells with damping characteristics. The next two equations implement the coefficients according to that characteristic:

$$S_{tex} = \frac{1}{N}\left(\frac{T_r}{1+11(I-1)^2}\right); \quad (11)$$

$$S_{tix} = \frac{1}{N}\left(\frac{-T_r}{1+11(I+1)^2}\right); \quad (12)$$

where T_r is the strength of the rate of change synapses.

The sensory and upper level signals, and the error and dynamic sensory signals converge to the output unit, whose output signal (O) will be the input to any kind of actuator. That output unit receives sensory information, upper level commands, and a combination of error and rates of change of the signals, and generates the output signal according to the following equation.

$$O = T_N \tanh\left[\alpha\left(\delta + \sum S_j + \sum S_k\right)\right] \quad (13)$$

where S_j and S_k are the outputs of the upper level and sensory motor unit synapses respectively, and δ is the signal generated in the inter-unit as a function of the error and rates of change.

The sensory and upper level signals are transmitted through two symmetrical (in terms of threshold and strength) sets of synapses, which are the synapses with plasticity that will be adjusted by learning. This solution resembles the mechanisms of sensitization, habituation and classical conditioning:

$$S_j = \frac{1}{N}\left(\frac{T_j}{1+a(I_c - I_{0,j})^2}\right); \quad (14)$$

$$S_k = \frac{1}{N}\left(\frac{T_k}{1+a(I_s - I_{0,j})^2}\right); \quad (15)$$

where S_j is the output of the *j-th* synapse connected with "the wish", S_k is the output of the *k-th* synapse connected with the actual condition signal, T_j and T_k are the strength of the *j-th* and of the *k-th* synapses respectively.

3. THE NATURAL CIRCULATION THERMAL HYDRAULIC LOOP

Figure 5 presents a schematic diagram of the Natural Circulation Loop (NCL), which resembles an Advanced Pressurized Water Reactor Emergency Heat Removal System. The NCL has an electric heater, that it is the hot source of the system, and a heat exchanger, that is the heat sink. The heat exchanger is made of two horizontal manifolds connected by a vertical tube bundle immersed in a water tank. Cold water coming from an elevated water reservoir is supplied to the water tank by gravity. A magnetic flow meter is installed in the main circuit line. The secondary cooling water flow is controlled by a globe valve and measured with a flow meter.

A numerical model was developed to simulate the thermal and hydraulic processes of the NCL. Figure 5 also presents some conventions used in the simulation model. Tables 1 and 2, show the parameters used in the model. A description of these parameters is found bellow. Although the model is simple it is able to simulate, with enough precision, the dynamics of the NCL. The basic assumptions used in the model are one-dimensional flow and incompressible fluid.

Mass conservation

For the mass conservation equation the water is considered an incompressible fluid. Thus, for one-dimensional flow, the mass conservation results in a constant mass flow rate throughout the whole loop at any instant. This result allows decoupling the continuity and momentum equations from the energy equation.

Energy conservation

In the energy balance the dissipation terms and the heat conduction through the water are neglected, so that the general energy equation for the fluid in a control volume is given by:

$$\rho A\frac{\partial T}{\partial t} = -\dot{m}C\frac{\partial T}{\partial s} - Pq'', \tag{16}$$

where ρ is the average water density in the volume, C is the water specific heat at constant pressure, T is the temperature, A is the flow area, $\dot{m}$ is the mass flow rate, s represents the dimension in the flow direction, P is the section perimeter, and q'' is the heat flux.

To distinguish between the two fluids in the heat exchanger, the water in the main loop is called primary fluid and the cooling water in the heat exchanger is called secondary fluid. With this convention the energy equation is applied to the NCL as described next.

The NCL is divided into regions. These regions are presented in Fig. 5, for example region 4 is denoted by R-4. Each region is further divided into several volumes. The general energy equation applied to the primary side results in following expression:

$$\rho_{r,i} V_{p,r,i} C\frac{\partial T_{p,r,i}}{\partial t} = -\dot{m}_p C\Delta s\frac{\partial T_{p,r,i}}{\partial s} - S_{p,r,i} q''_{p,r,i}, \tag{17}$$

where the subscript r defines the region, the subscript i denotes the volume, the subscript p specifies the primary side, Δs is the volume length, and S is the volume surface area. For the secondary side of the heat exchanger the energy equation is similar.

A heat transfer model provides the coupling between the primary and secondary fluids across the tube walls of the heat exchanger. An energy balance in the tube walls results in the following expression:

$$\rho_M V_M C_M \frac{\partial T_{M,r,i}}{\partial t} = S_{p,r,i} q''_{p,r,i} + S_{s,r,i} q''_{s,r,i}\,, \tag{18}$$

where the subscript M denotes the metal and, q''_p and q''_s are the wall heat fluxes at the primary and secondary sides respectively.

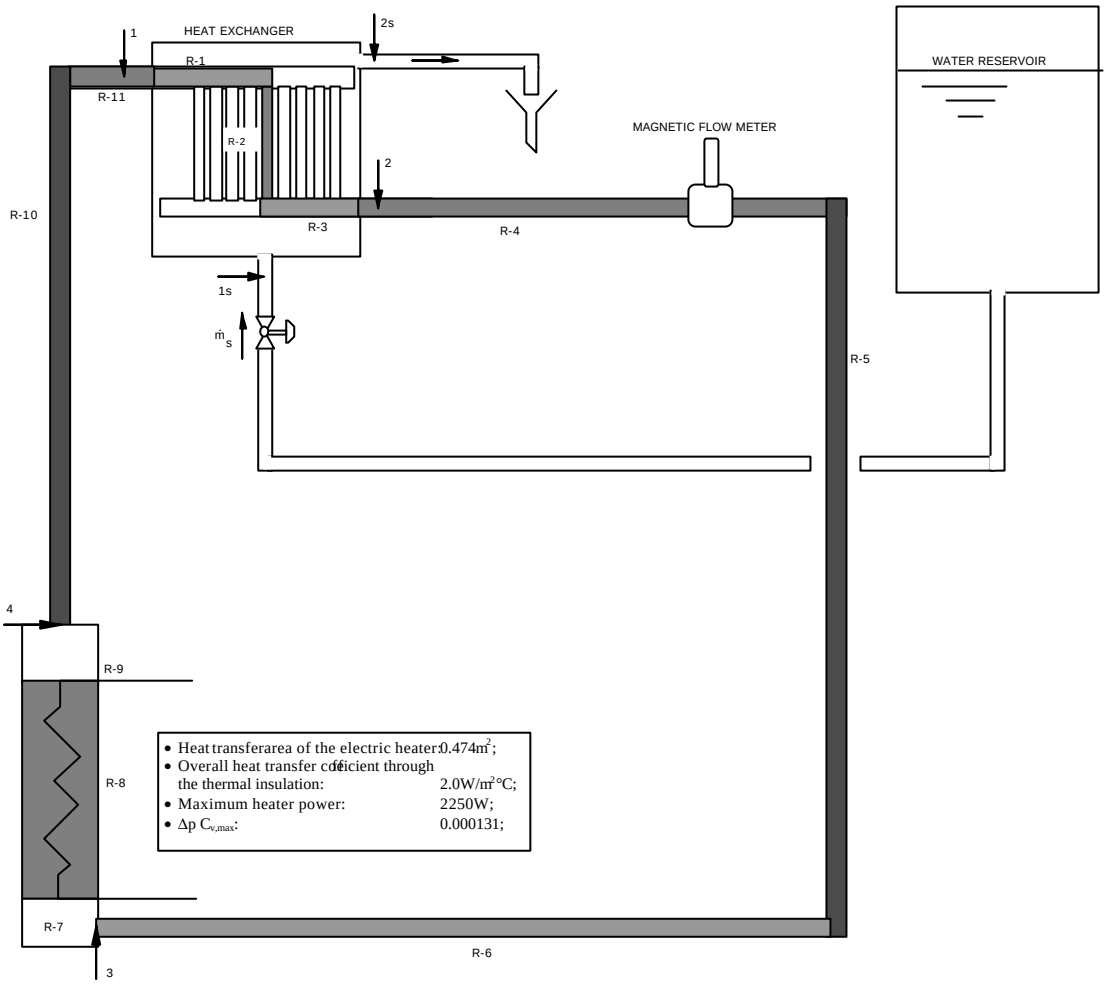

Figure 5 - Schematic of the Natural Circulation Loop (NCL).

Table 1 - NCL primary side hydraulic data.

Region	Control Volumes	D_H (m)	L_{EQ} (m)	Flow Area (m^2)	Volume (m^3)
1	5	0.0381	283.1	0.00114	0.00114
2	5	0.007945	179.9	0.0008924	0.000527
3	5	0.0381	223.1	0.00114	0.00114
4	5	0.0208	284.0	0.0003398	0.001018
5	10	0.0208	457.5	0.0003398	0.001642
6	5	0.0208	230.5	0.0003398	0.001417
7	2	0.0208	103.8	0.0003398	0.000027
8	5	0.0144	118.1	0.00188	0.00374
9	2	0.0144	58.9	0.00188	0.00033
10	8	0.0208	228.2	0.0003398	0.001224
11	2	0.0208	48.4	0.0003398	0.0000595

Table 2 - Heat exchanger secondary side data.

Parameter	Region 1	Region 2	Region 3
Heated perimeter (m)	0.13964	0.53863	0.13964
Heat transfer area (m^2)	0.13964	0.34203	0.13964
Flow area (m^2)	0.2056	0.2500	0.2056
Volume lengths - Δs (m)	0.100	0.127	0.100
h_p ($W/m^2\,^oC$)	500.0	645.0	500.0
h_s ($W/m^2\,^oC$)	500.0	645.0	500.0

The heat fluxes are given by the following equations:

$$q''_{p,r,i} = h_{p,r,i}(T_{p,r,i} - T_{M,r,i}); \quad (19)$$

$$q''_{s,r,i} = h_{s,r,i}(T_{M,r,i} - T_{s,r,i}); \quad (20)$$

where h_p is the heat transfer coefficient from the primary fluid to the tube wall, h_s is the heat transfer coefficient from the tube wall to the secondary fluid, and T_M is the temperature of the tubes metal. These heat transfer coefficients were obtained experimentally.

For the regions inside the electric heater, the heat generated by the electric resistance is completely transferred to the water, so that the term $S_{p,r,i}q''_{p,r,i}\,i$ represents the fraction of the electric heat generated inside the volume *i*. For the others primary side regions, the heat flux corresponds to the heat loss to the environment, which is calculated according to equation 19 and the next expression:

$$q''_{m,r,i} = U_{isol}(T_{M,r,i} - T_{env}); \quad (21)$$

where q''_m is the heat transferred from the tube wall to the environment, U_{isol} is the global heat transfer coefficient from the tube metal to the environment through the thermal insulation, T_{env} is the ambient temperature. The tube wall temperature, T_M, is calculated by an equation similar to equation (18).

Momentum conservation

For the momentum conservation, the difference in the water specific mass through the loop is considered, because in a natural circulation loop the flow is driven by the difference in the fluid density between the

ascending and the descending lines. The primary fluid mass flow rate is calculated by the momentum conservation equation, which is written for each pipe segment presented in Fig. 5. For the segment between 4 and 1, corresponding to the ascending line, this equation results in the following:

$$L_{41}\frac{d\dot{m}_p}{dt} = (p_4 - p_1) + \rho_A g(z_4 - z_1) - f_{41}\frac{L_{eq,41}}{D}\rho_A\frac{v_{41}^2}{2}, \quad (22)$$

where ρ_A is the water specific mass in the ascending line, L_{41} is the pipe length between points 4 and 1, p_4 and p_1 are the pressures in points 4 and 1 respectively, g is the gravity acceleration, z_4 and z_1 are the heights of point 4 and 1 respectively, f_{41} is the friction factor, $L_{eq,41}$ is the equivalent length for the pressure loss, D is the pipe hydraulic diameter (the internal pipe diameter), and v_{41} is the average water velocity between points 4 and 1. Observe that as the overall effect of acceleration along the circuit is canceled, the acceleration terms of the momentum equations were removed.

The momentum equations for the other segments are similar to equation (22). Summing all the momentum equations written for every segment, results in:

$$L\frac{d\dot{m}_p}{dt} = \left(\frac{z_4 + z_3}{2}\right)(\rho_A - \rho_D) + \left(\frac{z_1 + z_2}{2}\right)(\rho_D - \rho_A) - f\frac{L_{eq}}{D}\rho\frac{v^2}{2} \quad (23)$$

where L represents the total loop length, ρ_D is the water specific mass in the descending line, and the last term represents the total friction in the loop. The water specific masses in the heat exchanger and in the electric heater are assumed to be an average of the water specific masses in the ascending and in the descending pipes.

Cooling water control valve

The cooling water control valve regulates the secondary side mass flow rate. A generic valve model was considered to simulate the cooling water control valve behavior. This model relates the flow rate with the valve coefficient, C_v. The valve inlet and outlet pressures are considered to be constant, since the flow rate is small and the reservoir water level could be maintained constant. Therefore, the secondary side mass flow rate is given by the following equation:

$$\dot{m}_s = \rho_s A_v \Delta p C_v, \quad (24)$$

where ρ_s is the secondary side water specific mass, A_v is the valve flow area, and Δp is the pressure drop in the valve which is considered constant. The maximum C_v value was experimentally obtained. Its dependence with the valve flow area is modeled by:

$$C_v = (2.7A_v e^{-A_v})C_{v,\max}. \quad (25)$$

Numeric solution, parameters and NCL data

The equations that model the thermal and hydraulic processes of NCL are solved with the aid of a computer program. The time derivatives in the dynamic equations are approximated using the Euler Method. In the case of the temperatures this is:

$$T_{r,i}^{t+\Delta t} = T_{r,i}^{t} + \Delta t\frac{\partial T_{r,i}^{t}}{\partial t}; \quad (26)$$

where t is the time and Δt is the integration time step.

In the energy equations the space derivatives are approximated by the donor cell method. The solution of the dynamic processes follows a tandem approach, where the energy equations are solved first (using the previously determined flow rates) followed by the momentum equations. The solution of the energy equations begins at the heat exchanger primary water inlet, in the region numbered R-1. The solution of the energy equations follows the sequence of Fig. 5.

In the momentum equation, the water properties are evaluated at the water mean temperature in each region and not at the temperature in each control volume. As each region is uniformly divided into several control volumes of identical size, the region mean temperature is the arithmetic average of the temperatures of each control volume. The water physical properties are evaluated at these mean temperatures by means of temperature dependent functions.

The friction factor for Reynolds numbers greater than 100 was experimentally obtained, yielding:

$$f = 0.7 \times \Re e^{-0.25}; \tag{27}$$

for $Re \leq 100$ the friction factor is assumed to be constant and equal to 0.22.

The primary and secondary heat transfer coefficients of the heat exchanger were experimentally obtained. Overall heat transfer coefficients variations within a 15% range were observed in the initial phase of the experiments. This variation is considered small so that constant heat transfer coefficients for both the primary and secondary sides of the heat exchanger were used in the simulations. Table 2 shows the experimental values obtained for these coefficients, note that these values reproduce the experimental global heat transfer coefficient applied to the total heat transfer area (133 W/°C).

4. THE COUPLING OF THE NCL MODEL WITH MULSY NETWORK

The NCL control problem consists on the control of the primary water temperature at a given position in the loop acting only on the heater power. The secondary side water temperature and flow rate are assumed to be *disturbances* to the process. These variables are monitored by the neural network controller and used to adjust the magnitude of the power control signal. The solution of this problem requires an improvement of the Motor Control Unit of the MULSY Network presented in section 2.

To manage external disturbances the MULSY Network was modified to receive the secondary water inlet temperature and the cooling water valve flow area fraction. Fig. 6 shows the MULSY network with these modifications. In this new configuration, the control motor unit of Fig. 4 is linked to two parallel branches, which processes the disturbances signals. Each one of these branches has a set of plastic synapses. The expressions of these plastic synapses are exactly the same as the ones used for the wish and the actual signals, equations (14) and (15).

The $\boldsymbol{d}$ signal, composed by the combination of the error with the rate of change of the controlled temperature, is also used to modify the synaptic strength of these new sets of plastic synapses. The desired signal, I_c, is also used to provide the selective characteristic for the strength adjustment of these disturbance synapses. The output of the disturbances units are used to modulate the gain of the motor unit output (O) in order to generate the control signal, as follow:

$$S_c = O_1 O_2 O, \tag{28}$$

where S_c is the control signal and O, O_1 and O_2 are the outputs of the control units of Fig. 6.

In the NCL problem, the network considers only the first order variation of the error signal (1st order approximation). Higher order terms are neglected because of the huge inertia of this thermal loop. This large inertia, which can be observed in the great time constant of the NCL, eliminates fast variations.

Neural Network data

Table 3 presents the data used in the MULSY Neural Network of Fig. 6. These data are the same as the ones used in the case of the planar two-link manipulator controller of reference [1], except by the number of synaptic terminals and the values of some constants. The decay constant for adjustment of the plastic synapses strength, l, was reduced by a hundred times (from 10 to 0.1) to match with the process time constant, which is very slow for a natural circulation process. As long as a different number of synapses is used, the constant a_s of the facilitating synapses was quite different, see Baptista [7]. However, its relationship with the constant a of the plastic synapses is the same, i.e., $a_s/a = 144/28.8 = 100/20 = 5$. The constant T_C assumes two different values, either 0 or 0.1, to turn off the plasticity process in some instances, as explained in the training description.

5. RESULTS

The MULSY Network training is performed during the execution of action commands: *this is an unsupervised training method*. Desired temperatures and projected disturbances constitute the training universe. Different from the manipulator's case [1], there are three training data tables, one for each given variable: the desired temperature, the cooling water valve opening area and the inlet cooling water temperature. Tables 4 to 6 show the data sets - note that the training is developed in three stages. The effects of the three variables are not superposed, i.e., while training for one of the variables, the synaptic plasticity process of the branches associated with the others variables is blocked (no-plastic changes). This is done by setting $T_C = 0$.

Each stage of the training phase is divided into sessions, making possible to observe the learning progress. In the 1st stage the seven conditions specified in the Table 4 are submitted 3 times to the MULSY Network controller. This represented 3x7x14,400 = 302,400 seconds of process time. The 2nd stage consists on the repetition for 2 times the 9 conditions of Table 5, or 2x9x12,800 = 230,400 seconds of process time. In the 3rd and last stage the first session is accomplished with 10,800 seconds for the first condition and 3,600 seconds for each one of the other conditions. The second session considers 7,200 seconds for the first condition and again 3,600 seconds for the others. Thus, the last stage represents 1x10,800 + 1x7,200 + 2x9x3,600 = 82,800 seconds of process time. Therefore, the whole training phase represents a total of 615,600 seconds of simulate process, which is about 171 hours. After executing the three training stages, the strength of the synaptic contacts grew from the initial values (zero) to the values shown in Fig. 7 to 9.

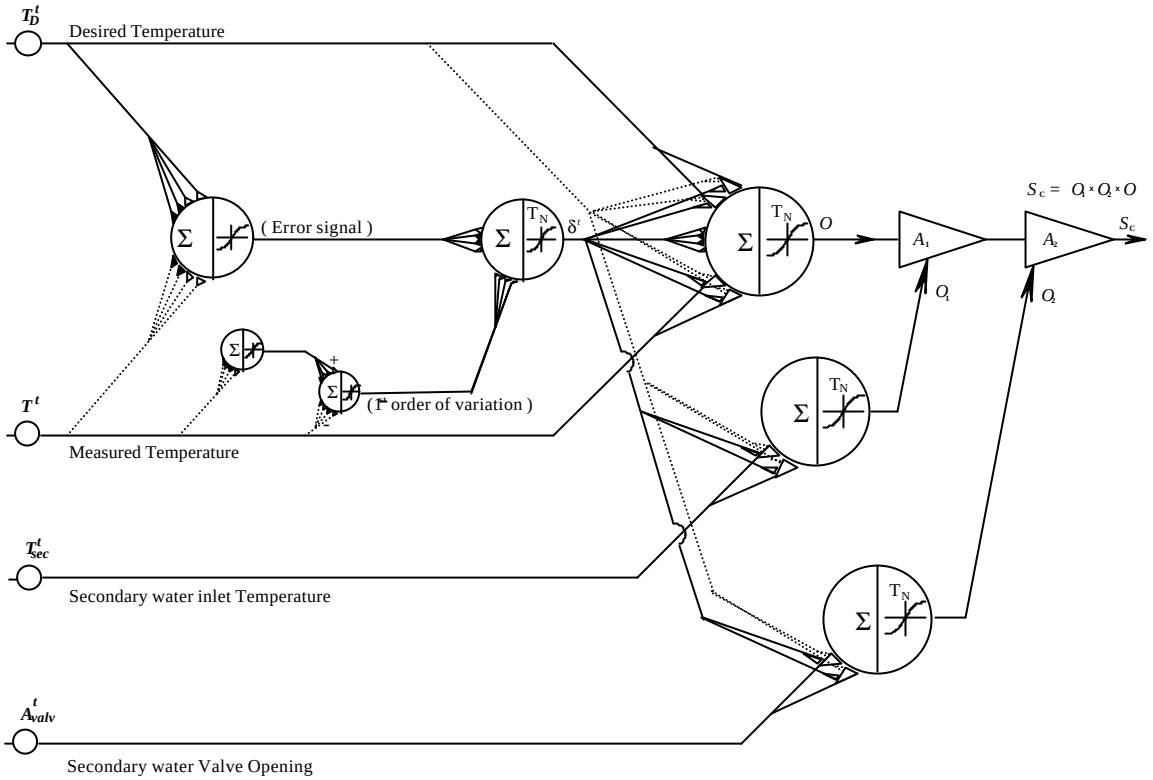

Figure 6 - MULSY N. N. controller with Disturbances Pathways.

Table 3 - Neural network data.

Parameter	Value
Unit's size - T_N	2.1
Units gain constant - a	0.5
Plastic synapse's constant – a	20.0
Plastic synapses in the sensory to output unit	13
Plastic synapses in the "wish" to output unit	13
Plastic synapses in the disturbance units	13
Consecutive thresholds interval in the plastic synapses ($\Delta I = I_{0,j+1} - I_{0,j}$)	0.2
Strength of error synapses – T_e	2.5
Strength of rates synapses – T_r	0.09
Strength of facilitating synapses – T_c	0 / 0.1
Synaptic strength decay constant - l	0.1
Plastic synapse's plastic constant – a_s	100.0

Table 4 – Training data for the *desired temperature*

Condition	Duration (s)	T_{env} (°C)	Cooling Temp.	Valve opening	**Desired Temp.**
1	14400.	25.0	20.0	0.25	**30.00**
2	14400.	25.0	20.0	0.25	**35.00**
3	14400.	25.0	20.0	0.25	**40.00**
4	14400.	25.0	20.0	0.25	**45.00**
5	14400.	25.0	20.0	0.25	**50.00**
6	14400.	25.0	20.0	0.25	**55.00**
7	14400.	25.0	20.0	0.25	**25.00**

Table 5 – Training data for the *cooling water temperature perturbation* (stage 2).

Condition	Duration (s)	T_{env} (°C)	**Cooling Temp.**	Valve opening	Desired Temp.
1	12800.	25.0	**14.0**	0.25	50.00
2	12800.	25.0	**16.0**	0.25	50.00
3	12800.	25.0	**18.0**	0.25	50.00
4	12800.	25.0	**20.0**	0.25	50.00
5	12800.	25.0	**22.0**	0.25	50.00
6	12800.	25.0	**24.0**	0.25	50.00
7	12800.	25.0	**26.0**	0.25	50.00
8	12800.	25.0	**28.0**	0.25	50.00
9	12800.	25.0	**30.0**	0.25	50.00

Table 6 - Training data for the valve *opening perturbation.*

Condition	Duration (s)	T_{env} (°C)	Cooling Temp.	Valve opening	Desired Temp.
1	1x10800 1x7200.	25.0	20.0	**0.05**	50.00
2	2x3600.	25.0	20.0	**0.10**	50.00
3	2x3600.	25.0	20.0	**0.15**	50.00
4	2x3600.	25.0	20.0	**0.20**	50.00
5	2x3600.	25.0	20.0	**0.25**	50.00
6	2x3600.	25.0	20.0	**0.30**	50.00
7	2x3600.	25.0	20.0	**0.35**	50.00
8	2x3600.	25.0	20.0	**0.40**	50.00
9	2x3600.	25.0	20.0	**0.45**	50.00
10	2x3600.	25.0	20.0	**0.50**	50.00

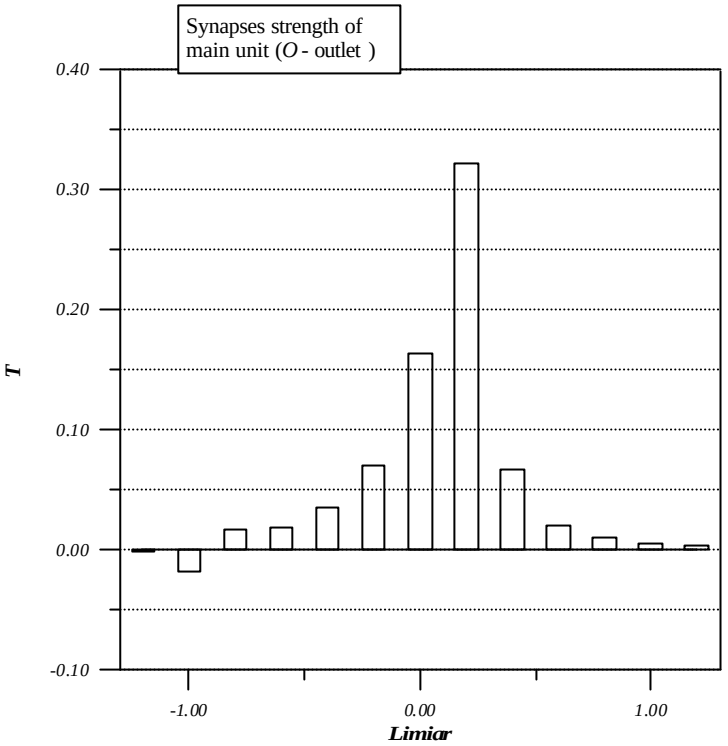

Figure 7 - Synaptic strengths after the 1st training stage.

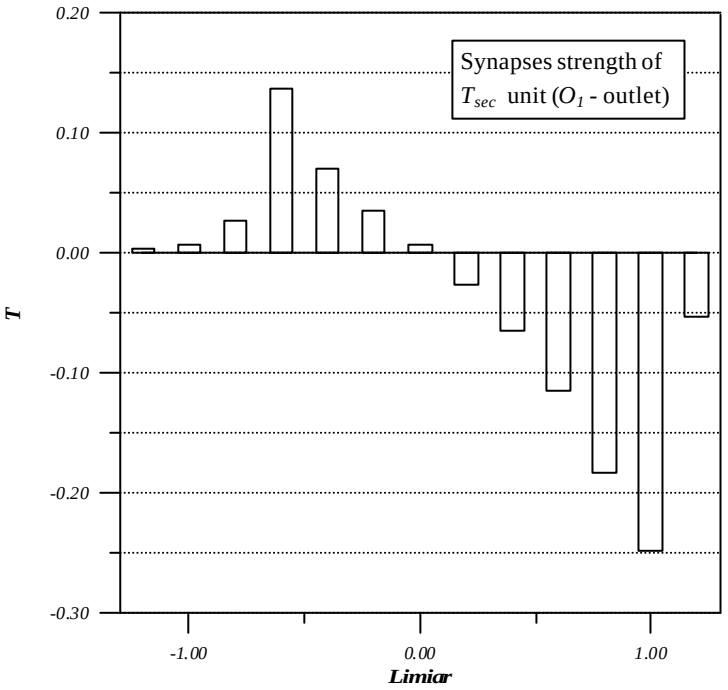

Figure 8 - Synaptic strengths after the 2nd training stage.

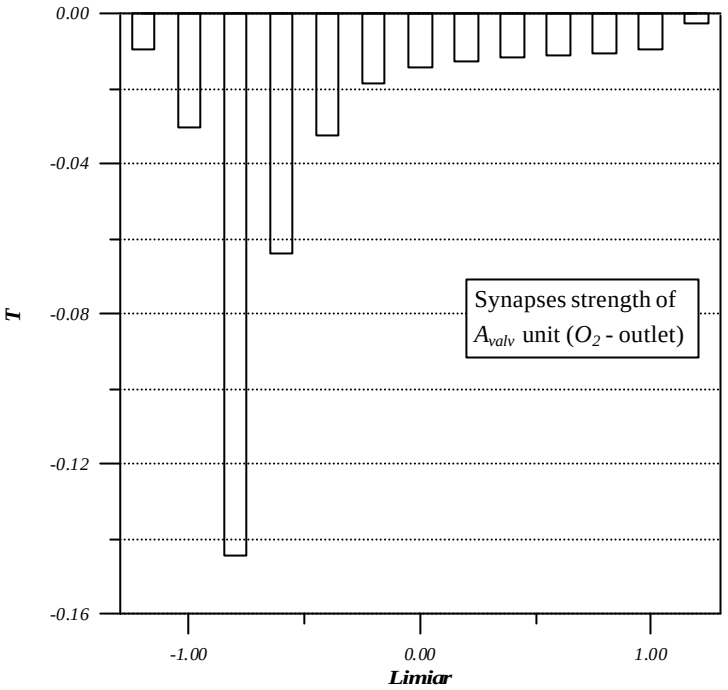

Figure 9 - Synaptic strengths after the 3rd training stage.

Performance tests

After the training, the MULSY Network controller was able to control the NCL primary water temperature under several conditions of disturbances in the cooling water valve opening and in the cooling water temperature. Tests were performed to evaluate the generalization capability of the network to execute commands that are not present in the training tables. During these tests, the plasticity mechanisms were blocked to avoid additional synaptic strength modification. The tests were executed on the physically possible domain, limited by the plant design.

The results of a single simulation test composed of several transient operations within a 26 hours period are presented. The test begins with the ambient temperature at 25°C and the cooling water temperature at 20°C. In the first command the desired primary side temperature is equal to the mean training conditions, i.e., 50°C at the heater outlet, with the cooling water valve opening corresponding to 25%. The test continues with the conditions shown in Table 7.

Table 7 - Performance test data set.

Condition	Duration (s)	T_{env} (°C)	Cooling Temp.	Valve Opening	Desired Temp.
1	16000.	25.0	20.0	0.25	50.00
2	7200.	25.0	23.0	0.25	50.00
3	7200.	25.0	25.0	0.25	50.00
4	7200.	25.0	25.0	0.25	55.00
5	7200.	25.0	25.0	0.12	55.00
6	7200.	25.0	25.0	0.08	55.00
7	7200.	25.0	25.0	0.08	60.00
8	7200.	25.0	25.0	0.08	33.00
9	7200.	25.0	15.0	0.08	33.00
10	7200.	25.0	15.0	0.08	53.00
11	7200.	25.0	15.0	0.08	42.00
12	7200.	25.0	17.0	0.33	37.00

The duration of the first condition was chosen to allow the NCL primary water temperature to approach almost a steady state condition. The natural circulation process in the NCL requires approximately 22,000 seconds (experimentally measured [11]) to reach a steady state condition in the heat exchanger secondary side. Note that 16,000 seconds is about the time to reach partial regime stability in the primary side of the heat exchanger, therefore this is the duration chosen for the first step. All the other steps last 7,200 seconds, which is about 1/3 of the time to reach stabilization, this leads to about 95% of the steady state primary side temperature. Figure 10 shows the tests conditions as a percentage of the mean training conditions (primary water temperature of 50°C, cooling water temperature of 20°C and valve opening fraction of 0.25). Observe that some values of Table 7 are out of the training set range, others are between two training values but not coincident with any one.

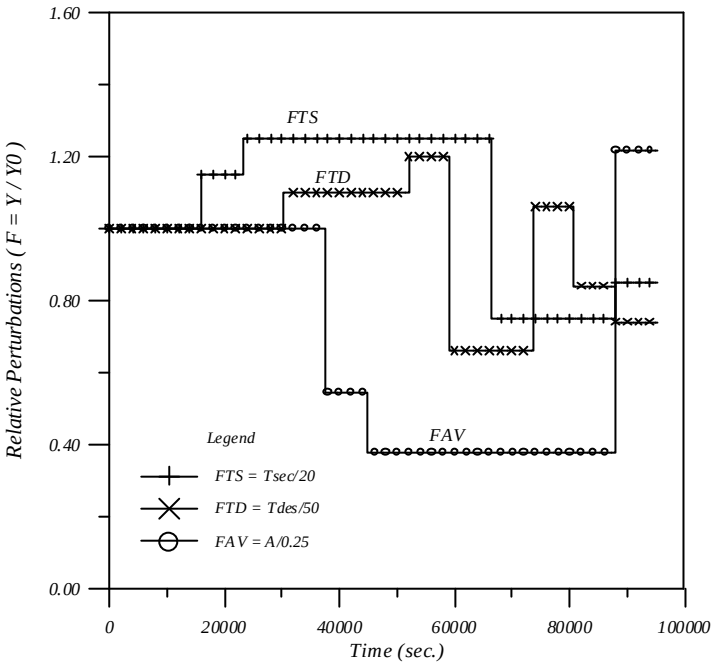

Figure 10 - Relative Perturbations.

The error in the desired temperature, defined as the difference between the observed and desired temperatures is presented in Fig. 11. Only in four instances the observed temperature errors were out of the range of ±0.5°C. Two of these instances happen when the time was not enough for the system to accommodate the perturbation. Another instance occurred when the two highest perturbations (cooling water temperature of 15°C and valve opening of 0.08) were combined, and the last instance happened when the valve opening of 0.08 was combined with a desired temperature 5°C over the maximum trained temperature.

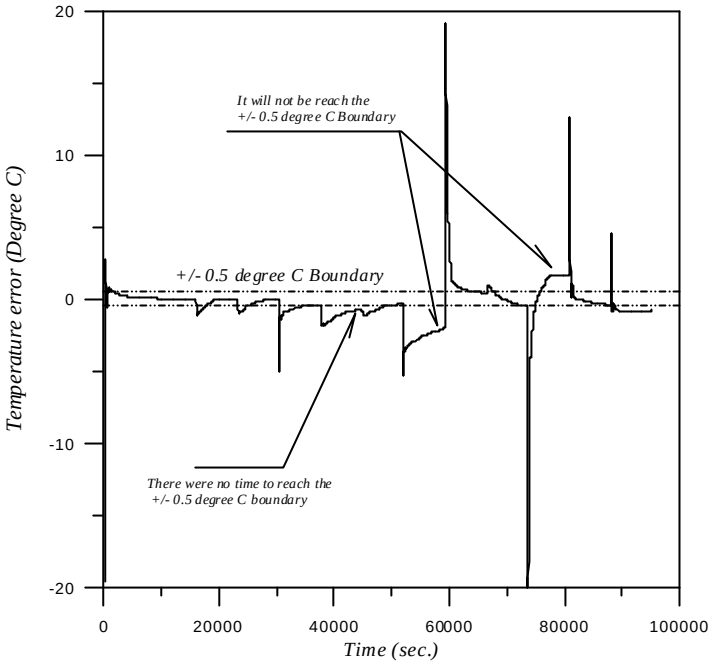

Figure 11 - Temperature error evolution.

5 – CONCLUSIONS

Previous works, [1] and [7], have demonstrated that the MULSY learning algorithm is stable and converges to a solution. These works demonstrate that MULSY training can result in the building of a *proportional derivative controller*, which provides a stable control. This work presents a review of the MULSY concept.

The MULSY concept is based on three principles: (1) the option of task-specific networks with the use of multiple contacts in the axon terminals which increases the integration capability of the network; (2) higher classes of connection's transfer functions improve the input-to-output relation, allowing a reduction in the total number of units with expensive sigmoidal functions, a network with only seven units was able to control a complex system such as the NCL; and, (3) the training task is performed without the need of input-output examples, i.e., the training is performed on-line, during the execution of desired commands, this is an unsupervised learning approach.

This work presents an improvement in the MULSY Neural Network concept to accommodate external perturbations. The results obtained in the NCL temperature control, even with perturbation conditions outside the training set, show that MULSY was able to generalize the learning. The good performance indicates that the MULSY, with this disturbance rejection scheme, can be easily implemented in the control of much kind of systems.

REFERENCES

[1] Baptista F., B.D.., Cabral, E.L.L., Soares, A.J., 1998, "A New Approach to Artificial neural Networks," *IEEE Transactions on neural Networks, Vol. 9, No. 6, pp. 1167-1179.*

[2] Kolen, J.F., Goel, A.K., 1991, "Learning in Parallel Distributed Processing Networks: Computational Complexity and Information Content", *IEEE Transactions on Systems, Man, and Cybernetics, Vol. 21, No. 2*.

[3] K. Akazawa and K. Kazunori, "Neural Network Model for Control of Muscle Force Based on the Size Principle of Motor Unit", *Proceedings of the IEEE, vol. 78, No. 9, September* 1990.

[4] C. J. DeLuca, R.S. LeFever, M.P. McCue, and A.P. Xenakis, "Controls Scheme Governing Concurrently Active Human Motor Units During Voluntary Contractions", *J. Physiol., vol. 329, pp. 129-142*, 1982.

[5] Kandel, E. R., Siegelbaum, Steven A. S., and Schwrtz, J. H., "Synaptic Transmission", *in Chap. 9, page 121 of "Principles of Neural Science"*, Third Edition, edited by Eric R. Kandel, James H. Schwartz, and Thomaz M. Jessel and published by Prentice-Hall International Inc., 1991.

[6] Weiss, P., and Hiscoe, H.B., "Experiments on the mechanism of nerve growth", *J. Exp. Zool., 107:315-395, 1948.*

[7] Baptista F., B. D., Redes Neurais Artificiais para Controle de Sistemas de Reatores Nucleares, São Paulo: 1998, Doctoral Thesis – Instituto de Pesquisas Energéticas e Nucleares, Universidade de São Paulo, (in Portuguese).

[8] Kandel, E. R., and Schwartz, J.H., "Molecular Biology of Learning: Modulation of Transmitter Release", *Science, 218, pp. 433-443, 1982*.

[9] Kandel, E.R., "Genes, Nerve Cells, and the Remembrance of Things Past", *J. Neuropsychiatry, vol. 1, pp.103-125, 1989*.

[10]E.R. Kandel, J.H. Schwartz and T.M. Jessel, *Principles of Neural Science*, Prentice-Hall International Inc., Third Edition, 1991.

[11]Macedo, L.A., "Control of Passive Emergency Cooling Systems of Nuclear Reactors by Bypass Lines", São Paulo: 2001, Master Degree Thesis – Instituto de Pesquisas Energéticas e Nucleares, Universidade de São Paulo, (in Portuguese).